does not provide any information on the mechanism because this bond is not as polar as the P–O bond. The vanadate is not a TSA in this aspect of its behavior.

To test the interaction with the His-119 residue, five points along the proton transfer curve from oxygen to nitrogen were calculated by using the model shown schematically in Figure 3. As seen in Figure 4 the energy curves for both P and V complexes are very similar. The similarity in the proton-transfer energetics occurs in spite of differences in the X–O(H) bond lengths between the P and V five-coordinate monoanions. The relative energy origin is arbitrarily set for the proton 1 Å from the nitrogen. As the proton is moved to the oxygen, it first passes through a maximum at about half the distance. The attraction of the dianion then takes over rapidly with the equilibrium position of the proton on the oxygen in this model. The binding energy to oxygen is relatively so large that it is evident that either the proton shuttles between equatorial and axial oxygen sites only within the influence of the His or large additional interactions must be considered for the proton to shuttle between the phosphorane TS and the His-119 residue as contemplated in the mechanism. An obvious candidate is the Asp-121 that is H-bonded to His-119.[23,24] The Asp stabilizes the protonated state of the His-119 but is not part of a charge relay.[24] In agreement with Umeyama[24] the present results suggest that the potential of the Asp is an important part of the mechanism if an initial proton transfer is required to neutralize the phosphate anion. Substituting Asn or a less polar group for Asp should inhibit the proton transfer from the TS and therefore the initial cyclization reaction. Stabilizing the vanadate monoanion would produce a structure closer to the TSA. Apparently the vanadate monoanion is the dominant species in solution,[4] suggesting the Asp is shielded from the monoanion. We conclude that the five-coordinate monoanion is both an electronic and a structural TSA with regard to interaction of His-119 with an equatorial oxygen ligand.

4. Conclusion

The five-coordinate vanadate inhibitor is found electronically to have both similarities to and differences from the phosphorane. The observed Lys-41 and His-12 orientations, which generated the initial interest, are not found relevant to the RNase A mechanism. Since the electrostatic potential at H-bonding distances of O–(V) for both monoanion and dianion vanadates are considerably smaller than expected for O–(P) in the transition-state phosphorane, the flexible Lys-41 side chain can search for and, apparently, bind to the more electronegative axial O–(H) site. The position of this residue is, therefore, not probing the electronic properties of the transition state and irrelevant to the mechanism but another indication of the flexibility of this side chain.

On the other hand, H-binding of His-119 to O–(H) probes the transition-state electronic behavior since the electrostatic behavior at all other oxygen sites is similar for the vanadate and phosphorane, and the stabilization of the vanadate dianion provides an electronic view of the dissociating phosphorus dianion. Although the variations in dianion bond distances can be probed as the calculated structure varies from the monoanion, the P dianion rapidly tends to a dissociating $H_2PO_4^-$. Observation of the vanadate dianion in the crystal is supported by the calculation of a stable and energetically favored vae intermediate. The observation of His-119 proximity to both axial and equatorial oxygens is suggestive of the relative flatness of the potential in this region. For static binding the axial oxygen has the larger electrostatic potential, which supports the observed orientation of the H-bond, but the His-119 can readily interact with the equatorial position if the potential alters during reaction. The importance of the observation of the dianion and the vae form of the dianion, though, is dependent on the extent to which the V and P dianions are analogous. An H-bond-stabilized vae P dianion should also be lowest in energy, suggesting the His-119 binding in the crystal structure is probing one of the steps in the hydrolysis of the phosphate. Modification of the protein to stabilize the monoanion vanadate would be of interest since the transition state occurs with this ionicity at an earlier stage in the mechanism.

Supplementary Material Available: Tables of Cartesian and internal coordinates of the equatorial–axial and equatorial–equatorial five-coordinate vanadate anions (2 pages). Ordering information given on any current masthead page.

(23) Deakyne, C. A.; Allen, L. C. *J. Am. Chem. Soc.* **1979**, *101*, 3951.
(24) Umeyama, H.; Nakagawa, S.; Fujii, T. *Chem. Pharm. Bull.* **1979**, *27*, 974.

Theoretical Determination of Partition Coefficients

Jonathan W. Essex,[†] Christopher A. Reynolds,[‡] and W. Graham Richards*,[†]

Contribution from Oxford Centre for Molecular Sciences, Physical Chemistry Laboratory, Oxford University, South Parks Road, Oxford OX1 3QZ, United Kingdom, and Department of Chemistry and Biological Chemistry, University of Essex, Wivenhoe Park, Colchester CO4 3SQ, United Kingdom. *Received August 28, 1991*

Abstract: The free energy perturbation method, implemented within a molecular dynamics framework, has been used to calculate differences in log *P*s between methanol, ethanol, and propanol partitioned between water and carbon tetrachloride. The calculated results agree with experiment to within 0.45 log *P* unit or about 3 kJ mol^{-1}. The difference in log *P* between methanol and ethanol was determined relatively easily. However, difficulties were experienced in extending the calculations to include the more flexible propanol molecule. A systematic variation of parameters was performed which highlighted the reason for the poor results, namely, the failure of the atomic charges to give a good description of the electrostatics in all conformations. This problem was overcome by using charges derived from the molecular electrostatic potential (MEP) for each conformation, weighted according to the appropriate Bolzmann population. It is proposed that these multiple conformation MEP derived charges will be useful in many other applications.

Introduction

Partition coefficients, which describe the partitioning of a solute between an organic and an aqueous phase, find extensive use in medicinal chemistry and drug design. It is often assumed that partition coefficients, and in particular those obtained for the water–octanol system, reflect the hydrophobicity of the solute molecule. The hydrophobicity is often used to describe the free energy changes involved in the movement of a drug from the aqueous phase to a lipid bilayer[1] but may also be important in the binding of the substrate to its macromolecular active site.

[†] Oxford University.
[‡] University of Essex.

(1) Hansch, C.; Dunn, W. J., III *J. Pharm. Sci.* **1972**, *61*, 1–19.

0002-7863/92/1514-3634$03.00/0

Partition coefficients are frequently involved in the determination of quantitative structure–activity relationships[2-6] which are used to correlate biological activity to these and other physical properties such as steric and electronic factors.

Because of the importance of partition coefficients to the above area of research, we have recently investigated the calculation of partition coefficients from computer simulations using the free energy perturbation method.[7] These calculations permit the difference in $\log_{10}$ of the partition coefficient (log P) to be determined from first principles by running computer simulations in which one compound is mutated into the other during the course of the simulation; the molecular dynamics simulations, in both the aqueous and organic phases, are based on a classical mechanical force field and treat all the atoms explicitly.

The initial work[7] considered the difference in log P between methanol and ethanol partitioned between water and carbon tetrachloride; this article considers the extension to propanol which is by no means trivial. While propanol merely represents an increase in the alkyl chain of only one methylene unit, the extension of the method to propanol involves extra degrees of freedom and requires the introduction of a new methodology to handle correctly the conformational dependence of the parameters. These calculations may also be seen as an extension of the log P calculations of Jorgensen since these considered rigid molecules.[8]

The free energy perturbation method[9] has now been applied to about 30 aqueous systems of real chemical or biological interest (as opposed to model systems studied for the purposes of methodological development), but to date there are only a relatively small number of reported free energy simulations in organic solvents (for examples, see refs 8 and 10–12). This article provides additional support for the usefulness of the free energy perturbation method in nonaqueous solvents as well as giving valuable insight into the related problem of extending a force field to molecules which were not in the original calibration set.

Methods

General. The partition coefficient of a compound, A, distributed between two immiscible solvents is defined as

$$P = [\mathrm{A}]_{\mathrm{organic}}/[\mathrm{A}]_{\mathrm{aqueous}} \tag{1}$$

where we have assumed that the activity coefficients are unity. Since it is an equilibrium constant, it can be related to the associated free energy change, ΔG_1, for the transfer of A from the aqueous phase to the organic phase; the difference in log P between A and B is then related to $\Delta G_1 - \Delta G_2$.

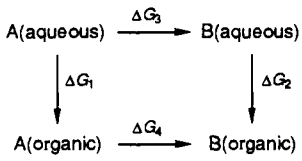

These phase transfer processes, ΔG_1 and ΔG_2, would be difficult to simulate using conventional molecular dynamics processes as they would involve desolvation and resolvation processes. However, the free energy perturbation method can be used to obtain the free energy change for the processes $A_{(solvent)} \rightarrow B_{(solvent)}$ by running a simulation in which A is gradually mutated to B. Since free energy is a state function, the difference in log Ps can readily be obtained from

$$-2.303RT\Delta \log P = \Delta G_1 - \Delta G_2 = \Delta G_3 - \Delta G_4 \tag{2}$$

The change ΔG_3 (or ΔG_4) is obtained from the exact free energy perturbation equation[13]

$$\Delta G = -RT \ln (\exp(-\Delta H_{AB}/RT))_A \tag{3}$$

which relates the difference in free energy, ΔG, between two systems A and B at a temperature T to ΔH_{AB}, the difference in the Hamiltonian, H, between the two systems. Here $\langle \ldots \rangle_A$ indicates that the average is evaluated over the ensemble of configurations generated according to the normalized probability distribution for system A. During this work, in order to ensure the rapid convergence of this average, the change A → B was split into 21 windows, each corresponding to an additional 5% change in the parameters of A to those of B. As in earlier work,[7,14] the configurations were generated using molecular dynamics. SHAKE[15] was employed to constrain the bond lengths, and thereby allow a time step of 0.002 ps to be used. The simulations were run at 293.15 K and 1 atm[16] since the most recent log P data were obtained under these conditions.[17] The water simulations were performed using a box of approximately 500 TIP3P water molecules with a nonbonded cutoff of 8 Å. The carbon tetrachloride simulations used approximately 200 molecules and a cutoff of 11 Å.

Parameters. The simulations were performed using the AMBER suite of programs,[18] AMBER was chosen because the force field[19-21] is well parameterized for biological molecules and because there are well-defined procedures for extending the force field to other types of molecules. Thus, the alcohol bond stretching, angle bending, torsional parameters, and nonbonding parameters were chosen by analogy with similar functional groups in the AMBER force field. The atom-centered charges were initially determined so as to reproduce the quantum mechanical molecular electrostatic potential (MEP) on a surface beyond the van der Waals surface, since this is the method used to determine the AMBER electrostatic parameters; these calculations were initially performed on the extended alcohol geometries using CHELP[22,23] interfaced to Gaussian 86.[24]

These parameters yielded poor results for ΔG_3 and Δ log P for the ethanol to propanol simulations, so a systematic variation of parameters was employed in order to locate the reasons for the errors. This systematic variation was guided by the OPLS alcohol parameters[25] which were found to yield results in good agreement with experiment.[26] This variation led to the identification of the electrostatics in the aqueous simulations as the major source of error and so the simulations were repeated using multiple conformation MEP derived atomic charges. The major advantage of the multiple conformation MEP derived charges is that they are valid across the range of conformations for which the MEP has been determined, and, the greater the Boltzmann factor for each conformation, the more accurately the electrostatic properties of that conformations are reproduced. The theoretical basis of the multiple conformation MEP

(2) Tute, M. S. *Adv. Drug Res.* **1971**, *6*, 1–77.
(3) Martin, Y. C. *Quantitative Drug Design: A Critical Introduction*; Marcel Dekker: New York, 1978.
(4) Sandler, M.; Smith, H. J. *Design of Enzyme Inhibitors as Drugs*; Oxford University Press: Oxford, 1989.
(5) Taylor, J. B.; Kennewell, P. D. *Introductory Medicinal Chemistry*; Ellis Horwood Ltd: Chichester, 1981.
(6) Barlow, R. B. *Quantitative Aspects of Chemical Pharmacology*; Croom Helm Ltd: London, 1980.
(7) Essex, J. W.; Reynolds, C. A.; Richards, W. G. *J. Chem. Soc., Chem. Commun.* **1989**, 1152–1154.
(8) Jorgensen, W. L.; Briggs, J. M.; Contreras, M. L. *J. Phys. Chem.* **1990**, *94*, 1683–1686.
(9) Beveridge, D. L.; DiCapua, F. M. *Annu. Rev. Biophys. Biophys.* **1989**, *18*, 431–492.
(10) Rao, B. G.; Singh, U. C. *J. Am. Chem. Soc.* **1991**, *113*, 4381–4389.
(11) Mazor, M. H.; McCammon, J. A.; Lybrand, T. P. *J. Am. Chem. Soc.* **1989**, *111*, 55–56.
(12) Rao, B. G.; Singh, U. C. *J. Am. Chem. Soc.* **1990**, *112*, 3803–3811.
(13) Zwanzig, R. W. *J. Chem. Phys.* **1954**, *22*, 1420–1426.
(14) Reynolds, C. A. *J. Am. Chem. Soc.* **1990**, *112*, 7545–7551.
(15) van Gunsteren, W. F.; Berendsen, H. J. C. *Mol. Phys.* **1977**, *34*, 1311–1327.
(16) Berendsen, H. J. C.; Postma, J. P. M.; van Gunsteren, W. F.; DiNola, A.; Haak, J. R. *J. Chem. Phys.* **1984**, *81*, 3684–3690.
(17) Korenmann, I.; Chernorukova, Z. *Zh. Prikl. Khim.* **1975**, *47*, 2595.
(18) Singh, U. C.; Weiner, P. K.; Caldwell, J. W.; Kollman, P. A. *AMBER* (Version 3.1); Department of Pharmaceutical Chemistry, University of California: San Francisco, 1988.
(19) Weiner, S. J.; Kollman, P. A.; Case, D. A.; Singh, U. C.; Ghio, C.; Algona, G.; Profeta, S., Jr.; Weiner, P. *J. Am. Chem. Soc.* **1984**, *106*, 765–784.
(20) Weiner, S. J.; Kollman, P. A.; Nguyen, D. T.; Case, D. A. *J. Comput. Chem.* **1986**, *7*, 230–251.
(21) Singh, U. C.; Kollman, P. A. *J. Comput. Chem.* **1984**, *5*, 129–145.
(22) Chirlian, L. E.; Francl, M. M. *QCPE Bull.* **1987**, *7*, 39; QCPE 524; CHELP.
(23) Chirlian, L. E.; Francl, M. M. *J. Comput. Chem.* **1987**, *8*, 894–905.
(24) Frisch, M. J.; Binkley, J. S.; Schlegel, H. B.; Ragavachari, K.; Melius, C. F.; Martin, R. L.; Stewart, J. J. P.; Bobrowicz, F. W.; Rohlfing, C. M.; Kahn, L. R.; Defrees, D. J.; Seeger, R.; Whiteside, R. A.; Fox, D. J.; Fleuder, E. M.; Pople, J. A. *GAUSSIAN 86*; Carnegie-Mellon Quantum Chemistry Publishing Unit: Pittsburgh, PA, 1984.
(25) Jorgensen, W. L. *J. Phys. Chem.* **1986**, *90*, 1276–1284.
(26) King, P. M.; Reynolds, C. A.; Essex, J. W.; Worth, G. A.; Richards, W. G. *Mol. Simulations* **1990**, *5*, 265–275.

Table I. Solvation Free Energy (ΔG_{sol}) and log P Differences for Methanol → Ethanol and Ethanol → Propanal Perturbations (Free Energies Are Given in kJ mol^{-1})

simulation no.	perturbation	charges method	van der Waals	torsional parameters	ΔG_{aq} (ΔG_3)^f	ΔG_{CCl_4} (ΔG_4)^f	Δ log P
1	MeOH → EtOH	3-21G MEP	AMBER	AMBER	−1.01 ± 0.68	−4.29 ± 1.11^6	−0.58 ± 0.23
2	MeOH → EtOH	OPLS	OPLS	OPLS	−2.17 ± 0.89	−5.10 ± 1.43	−0.52 ± 0.30
3	MeOH → EtOH	OPLS	OPLS[a]	OPLS	2.19 ± 1.29	−5.10 ± 1.43	−1.30 ± 0.34
4	MeOH → EtOH	6-31G* MEP	AMBER	AMBER	−0.68 ± 1.52	−4.17 ± 1.93	−0.62 ± 0.44
5	MeOH → EtOH	multi 3-21G MEP	AMBER	AMBER	2.62 ± 0.91	−4.49 ± 1.91	−1.27 ± 0.38
6	MeOH → EtOH	multi 6-31G* MEP	AMBER	AMBER	1.14 ± 1.20	−4.54 ± 1.20	−1.01 ± 0.30
7	EtOH → PrOH	3-21G MEP	AMBER	AMBER	−6.01 ± 0.91	−5.88 ± 1.75^6	0.02 ± 0.35
8	EtOH → PrOH	3-21G MEP	AMBER[a]	AMBER	−8.66 ± 0.23	−5.88 ± 1.75^6	0.50 ± 0.31
9	EtOH[b] → PrOH	3-21G MEP	AMBER	AMBER	−6.43 ± 0.43	−7.65 ± 1.21	−0.22 ± 0.23
10	EtOH → PrOH	6-31G* MEP	AMBER	AMBER	−6.93 ± 0.55	−5.57 ± 0.63	0.24 ± 0.15
11	EtOH → PrOH	OPLS	OPLS	OPLS	−2.07 ± 1.27	−5.98 ± 1.74^3	−0.70 ± 0.38
12	EtOH → PrOH	OPLS	OPLS[a]	OPLS	0.66 ± 0.17	−5.98 ± 1.74^3	−1.18 ± 0.31
13	EtOH → PrOH	3-21G MEP(united)	AMBER	OPLS	−5.26 ± 0.21		
14	EtOH → PrOH	3-21G MEP(united)	AMBER	AMBER	−5.13 ± 1.86^3		
15	EtOH → PrOH	3-21G MEP	AMBER	OPLS	−7.08 ± 1.21	−4.75 ± 0.27	0.42 ± 0.22
16	EtOH → PrOH	3-21G MEP	OPLS	AMBER	−7.27 ± 0.71		
17	EtOH → PrOH	3-21G MEP	OPLS[a]	AMBER	−7.83 ± 1.58		
18	EtOH → PrOH	OPLS	AMBER	AMBER	−1.15 ± 0.23	−4.38 ± 0.39	−0.58 ± 0.08
19	EtOH → PrOH	OPLS	AMBER	OPLS	−1.82 ± 0.27	−5.00 ± 0.27	−0.57 ± 0.07
20	EtOH → PrOH	multi 3-21G MEP	AMBER	AMBER	2.70 ± 1.45	−4.88 ± 0.80	−1.35 ± 0.30
21	EtOH → PrOH	multi 6-31G* MEP	AMBER	AMBER	1.55 ± 1.20	−4.24 ± 0.85	−1.03 ± 0.26
22	EtOH → PrOH	3-21G MEP[c]	AMBER	AMBER	1.81 ± 1.22	−5.88 ± 1.75	−1.37 ± 0.38
23	EtOH → PrOH	3-21G MEP[d]	AMBER	AMBER	1.81 ± 1.22	−4.88 ± 1.75	−1.19 ± 0.26
(24)	MeOH → EtOH	experiment			0.28 ± 1.53	−3.65[e]	−0.70
(25)	EtOH → PrOH	experiment			0.69 ± 1.50	−2.56[e]	−0.58

[a] No 12-6 van der Waals parameters used for the TIP3P water hydrogen atoms. [b] Simulation time double standard protocol. [c] Alternative dipole constraint charges; the value of ΔG_{CCl_4} given was obtained using single MEP charges. [d] Alternative dipole constraint charges; the value of ΔG_{CCl_4} given was obtained using multiple MEP charges. [e] Determined from ΔG_3 and Δlog P. [f] If more than two simulations were performed, the number is shown as a superscript.

derived charges is described fully in the preceding article.[27] Alternative dipole constrained charges were also used for the ethanol to propanol simulations; these charges are also fully described in the forthcoming article.

The AMBER force field was originally developed using charges derived from the STO-3G basis set.[28] However, in this work we have used charges derived using the 3-21G and 6-31G* basis sets[29,30] since these (particularly the 6-31G* basis set) give a more accurate description of the electrostatic properties of the molecules. Elsewhere we have found that free energy can vary widely with the basis set used to generate the charges,[31] and so a reasonably flexible basis set is essential. Moreover, the 6-31G* basis set is believed to yield charges that are more balanced[32] vis-à-vis the TIP3P water model[33] which was used in these studies. The TIP3P water model was used since it has yielded free energy differences in good agreement with experiment in many studies; for examples, see refs 34–38. The TIP3P water molecule does not contain a 12-6 repulsion dispersion term on hydrogen atoms, whereas the AMBER force field normally includes such functions on the hydrogen atoms; for the interaction between the TIP3P water and the alcohols, this term was normally included although it was excluded in some simulations.

The carbon tetrachloride parameters were taken from McDonald,[39] with the charges adopted by Bermejo,[40] for consistency with earlier work and because these parameters have successfully reproduced both structural and thermodynamic properties of liquid carbon tetrachloride. The carbon tetrachloride parameters differ from those used by Singh in a recent free energy perturbation study of solvation in carbon tetrachloride[10] in that our R^* parameters for C and Cl are larger and the bond polarity is reversed. Our electrostatic description is in line with experiment and quantum mechanical results using large basis sets with and without the inclusion of electron correlation. However, Evans[41] ignored the charges on carbon tetrachloride since the lowest multipole is an octapole and so the properties of carbon tetrachloride are probably not too dependent upon an accurate description of the electrostatics.

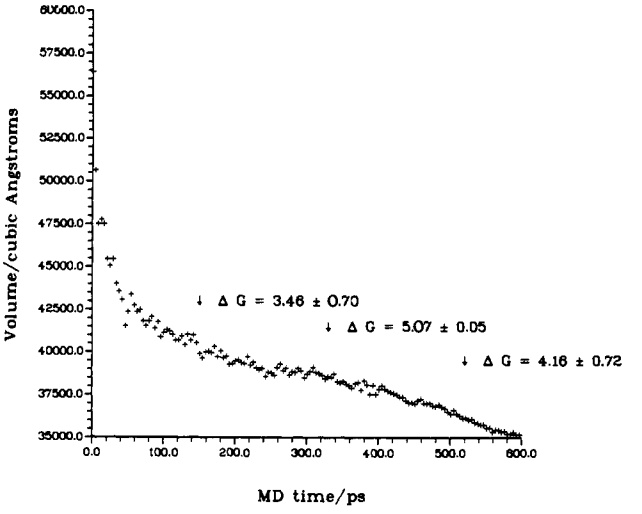

Figure 1. The variation in CCl_4 box volume with simulation time; the arrows mark the start times for the three independent EtOH → PrOH simulations which used 6-31G* multiple conformation MEP derived charges. The free energy change is also shown; the average of these values is given as simulation 21 in Table I.

(27) Reynolds, C. A.; Essex, J. W.; Richards, W. G. *J. Am. Chem. Soc.*, submitted for publication.
(28) Hehre, W. J.; Stewart, R. F.; Pople, J. A. *J. Chem. Phys.* **1969**, *51*, 2657–2664.
(29) Binkley, J. S.; Pople, J. A.; Hehre, W. J. *J. Am. Chem. Soc.* **1980**, *102*, 939–947.
(30) Hariharan, P. C.; Pople, J. A. *Theor. Chim. Acta* **1973**, *28*, 213–222.
(31) Lister, S. G.; Reynolds, C. A.; Richards, W. G. *Int. J. Quant. Chem.* **1992**, *41*, 293–310.
(32) Dang, L. X.; Kollman, P. A. *J. Am. Chem. Soc.* **1990**, *112*, 5716–5720.
(33) Jorgensen, W. L.; Chandrasekhar, J.; Madura, J. D.; Impey, R. W.; Klein, M. L. *J. Chem. Phys.* **1983**, *79*, 926–935.
(34) Cieplak, P.; Bash, P.; Singh, U. C.; Kollman, P. A. *J. Am. Chem. Soc.* **1987**, *109*, 6283–6289.
(35) Rao, S. N.; Singh, U. C.; Bash, P. A.; Kollman, P. A. *Nature* **1987**, *328*, 551–554.
(36) Singh, U. C.; Brown, F. K.; Bash, P. A.; Kollman, P. A. *J. Am. Chem. Soc.* **1987**, *109*, 1607–1614.
(37) Tidor, B.; Karplus, M. *Biochemistry* **1991**, *30*, 3217–3228.
(38) Ha, S.; Gao, J.; Tidor, B.; Brady, J. W.; Karplus, M. *J. Am. Chem. Soc.* **1991**, *113*, 1553–1557.
(39) McDonald, I. R.; Bounds, D. G.; Klein, M. L. *Mol. Phys.* **1982**, *45*, 521–542.
(40) Bermejo, F. J.; Eniciso, E.; Alonso, J.; Garcia, N.; Howells, W. S. *Mol. Phys.* **1988**, *64*, 1169–1184.
(41) Evans, M. W. *J. Chem. Phys.* **1987**, *86*, 4096–4101.

Since the poor agreement between calculated and experimental values for ΔG_3 (EtOH → PrOH) is closely correlated with the breakdown in the conformational behavior of the dipole, it was necessary to monitor the dihedral transitions about the O–C_α and C_α–C_β bonds of propanol in the course of a molecular dynamics simulation.

Equilibrium, Data Collection, and Convergence. Prior to data collection using eq 3, the system was equilibrated for between 10 and 200 ps; the actual simulations were run for 42 ps, apportioned approximately equally between equilibration and data collection (although some simulations were run for 84 ps to check for convergence). Recent research[42-45] suggests that simulation times greater than 100 ps and preferably 200–400 ps are required for a tight convergence of eq 3. It has also been suggested that tighter convergence is obtained from one long run rather than from the average of two shorter simulations.[42] In this study it was necessary to run six simulations for the process MeOH → EtOH and 16 simulations for the process EtOH → PrOH, and so it was not possible to run many very long simulations. However, where similar simulations give similar results, this may be taken as evidence of convergence, and in every case the $\Delta G_{solution}$ given in Table I is an average of at least two and in some cases three 42-ps simulations.

Some difficulty was observed in equilibrating the box of carbon tetrachloride containing propanol since a rapid decrease in volume was observed over the first 100 ps, followed by a gradual decrease over the subsequent 500 ps. The long relaxation time is no doubt due to the quasi-crystalline structure of liquid carbon tetrachloride. In view of this, the volume dependency of ΔG_4 was studied (see Figure 1), but since no clear trends were observed, it was assumed that ΔG_4 is independent of the box size. The value of ΔG_4 in simulation number 21 is the average of the three values given in Figure 1.

In view of the problem associated with the quasi-crystalline nature of liquid carbon tetrachloride, it may be preferable from a computational point of view to determine the log *P*s for chloroform which does not have a quasi-crystalline liquid structure, especially as chloroform is a more useful solvent. However, chloroform is more miscible with water than is carbon tetrachloride, and so from this point of view it is easier to reproduce the carbon tetrachloride experimental conditions.

Results and Discussion

Methanol–Ethanol log *P* Differences. Simulations 1–6 show that reasonable log *P* results may be obtained for this system using a variety of different parameter sets. In the forthcoming article we arbitrarily define good results as within 4 kJ mol^{-1} of experiment and it would seem appropriate to retain this criterion. It would not seem unreasonable to claim this accuracy for this very simple perturbation, namely, the growth of a methyl group from a hydrogen atom. The fact that all the different parameter sets yield good results suggests that the basic hydrogen to methyl mutation is easy to parameterize. However, as discussed in the next section, this is not always the case; the ethanol to propanol mutation is very sensitive to the choice of parameters and this suggests that additional factors are affecting this mutation.

Identifying the Source of Errors in the Propanol Simulations. Simulations 7, 8, and 10 show that the standard MEP calculations give poor results for both ΔG_3 and Δ log *P*, while simulations 11 and 12 show that the OPLS calculations are consistent with the experimental values. The Δ log *P* result for simulation 9 is in reasonable agreement with the experimental data quoted in Table I, although the quality of these data will be called into question below. Moreover, the value of ΔG_3 disagrees with experiment, and we therefore consider the satisfactory Δ log *P* fortuitous. The OPLS alcohol force field treats the $-CH_2-$ and $-CH_3$ groups as a single united atom, and so single conformation MEP derived united atom charges were generated for ethanol and propanol; simulations 13 and 14 show that the good results in simulations 11 and 12 are not an artifact arising from the use of a united atom force field. The torsional parameters are not the main source of error as is shown in simulations 13 and 15 where the AMBER torsional parameters were replaced by OPLS torsional parameters. For simulations 16 and 17, the AMBER van der Waals parameters were replaced by the equivalent OPLS parameters, but again this is not the source of the error. For simulations 18 and 19, the AMBER electrostatic parameters were replaced by the OPLS united atom charges; both of these simulations gave a vastly improved value of ΔG_3 and Δ log *P*. Moreover, columns six and seven of Table I show that the error not only lies with the electrostatic parameters, but also that this error affects primarily the aqueous simulations. Simulations 20 and 21 show that this error can be corrected by using the multiple conformation MEP charges described in the preceding article. Simulation 22 shows that reliable results can also be obtained using the alternative methodology of dipole constrained charges, also described in the preceding article.

Simulations 20–22 give Δ log *P* (EtOH → PrOH) values of −1.35, −1.03, and −1.37 for the 3-21G multiple conformation MEP, 6-31G* multiple conformation MEP, and 3-21G dipole constrained charge, respectively, in good agreement with the experimental Δ log *P* value given in Table I of −0.58 log *P* unit. Moreover, the values for ΔG_3 are also in good agreement with experiment. Simulations 5 and 6 and also 20 and 21 show that the quantum mechanically more reliable 6-31G* based results are superior to the 3-21G based results. The 6-31G* multiple conformation MEP results are within 0.45 log *P* unit of the experimental value; although this agreement with experiment is very good; it has to be seen alongside a proper assessment of the experimental results.

Assessing the Experimental Results. The experimental log *P* results given in Table I are the most recent ones for normal alcohols and are all taken from the same source.[17] For methanol, Korenmann[17] gives a log *P* value of −2.10. For ethanol, *K*oremann gives −1.40, Hanssens[46] gives −2.93, Bugarszky[47] gives −1.61, and Kuznetsova[48] gives −1.74. For propanol, two values are given: −0.82 (Korenmann) and −0.93 (Hanssens). Thus Korenmann gives a Δ log *P* (EtOH → PrOH) value of −0.58 while Hanssens gives −2.00. The single conformation MEP results are well outside this range, while the multiple conformation MEP results lie in the middle of this range. This illustrates a problem frequently encountered in applied computational chemistry, namely, that the reliability of experimental data against which calculations can be calibrated cannot always be assured. As a consequence of this, there may be cases where free energy perturbation methods could give results of comparable or superior quality to experiment. The experimental values for the free energies of hydration[49] given in Table I have been corrected to 293.15 K using enthalpy data.

Electrostatic and Conformational Properties of Propanol. The improved agreement with experiment may be taken as some justification for the use of multiple conformation MEP derived charges, but their primary justification lies in the fact that they are based on all relevant conformations and as a result correctly describe the variation of the electrostatic properties (particularly the dipole) with conformation. In the forthcoming article the Born equation is used to relate the error in ΔG_3 and ΔG_4 to the error in the dipole, and it was shown that the errors in ΔG_3 and ΔG_4 were comparable with the errors arising from the exaggerated dipole; this arose from the single conformation MEP charges and was observed in certain conformations – particularly the g_+ g_- conformation. Figure 2 shows the symmetrized distribution of propanol conformations for the multiple conformation MEP charges over a 40-ps time period and shows that the g_+ g_- conformation was indeed well sampled, giving further evidence that this conformation was indeed a major source of errors. Similar results, not shown, confirm that this conformation was indeed well sampled during the corresponding single conformation MEP propanol simulations.

In the forthcoming article it is shown that simulations based on restricted conformations were able to yield good values of

(42) Mitchell, M. J.; McCammon, J. A. *J. Comput. Chem.* **1991**, *12*, 271–275.
(43) Mazor, M.; Pettitt, B. M. *Mol. Simulations* **1991**, *6*, 1–4.
(44) Pearlman, D. A.; Kollman, P. A. *J. Chem. Phys.* **1991**, *94*, 4532–4545.
(45) Mark, A. E.; van Gunsteren, W. F.; Berendsen, H. J. C. *J. Chem. Phys.* **1991**, *94*, 3808–3816.
(46) Hanssens, I.; Mullens, J.; Deneuter, P.; Huyskens, P. *Bull. Soc. Chim. Fr.* **1968**, 3942–3945.
(47) Bugarszky, S. *Z. Phys. Chem.* **1910**, *71*, 753.
(48) Kuznetsova, E. M.; Gurarii, L. L. *Russ. J. Phys. Chem.* **1971**, *45*, 1761–1763.
(49) Cabani, S.; Gianni, P.; Mollica, V.; Lepori, L. *J. Solution Chem.* **1981**, *10*, 563–595.

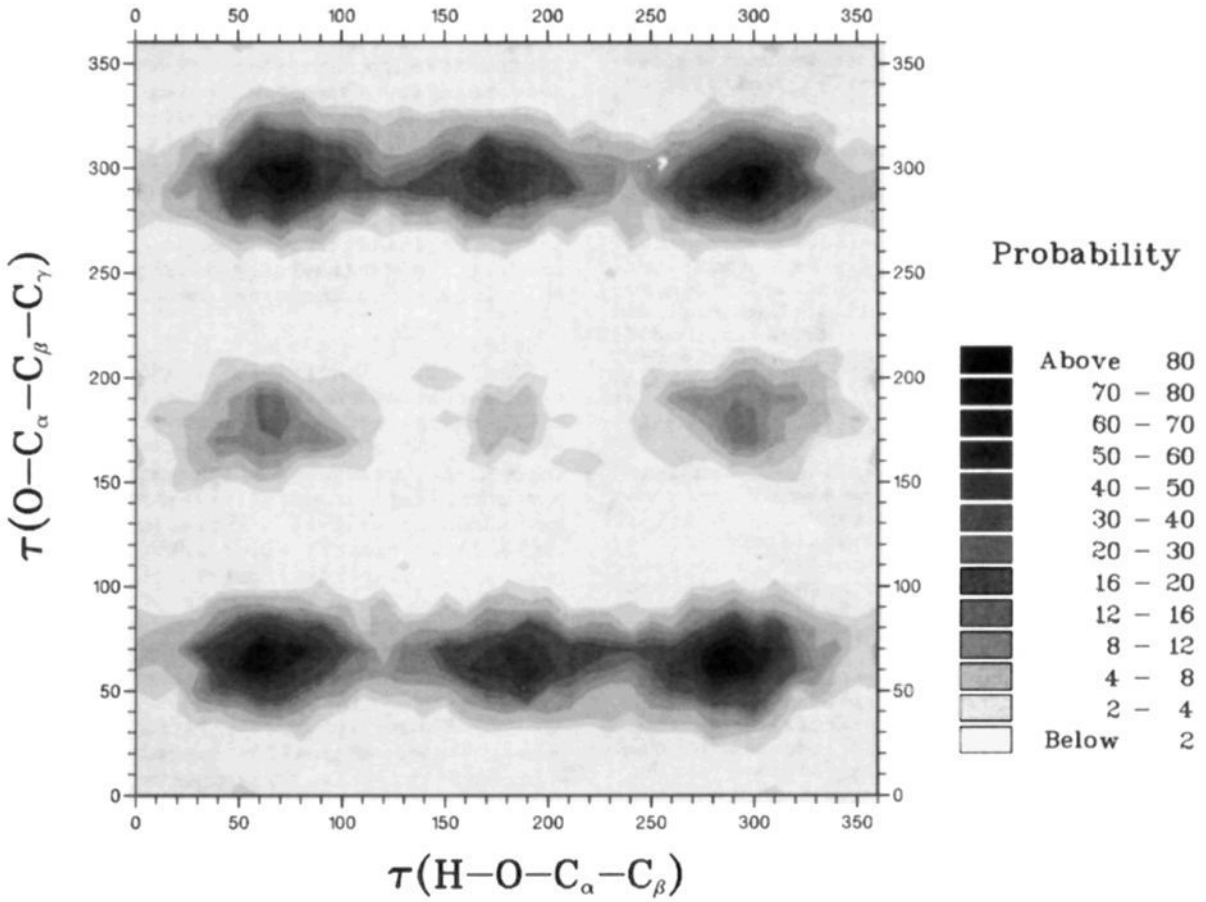

Figure 2. Unnormalized, symmetrized distribution of propanol conformations for a 40-ps simulation using 6-31G* multiple conformation MEP derived charges.

hydration free energies; this suggests that one possible reason for the error was that the propanol was sampling inappropriate regions of phase space. However, the similarity in the propanol conformational maps, generated using single and multiple conformation MEP charges, confirms that the error was not due to sampling the wrong region of phase space, but rather due to the breakdown in the electrostatics in certain conformations. The multiple conformation MEP charges were based on the gas phase Boltzmann probabilities; Figure 2 shows that a similar range of probabilities was also observed in solution, giving further evidence that the multiple conformation MEP charges are valid in solution and that there is not a serious weighting mismatch between the gas phase and solution phase.

One possible protocol for avoiding the errors introduced by single conformation MEP charges is to impose a rigid geometry on the solute. As indicated in the forthcoming article, this method may yield some success. Indeed, Jorgensen has shown that chloroform–water partition coefficients can indeed be calculated for rigid solutes (formally containing one torsional degree of freedom) using Monte Carlo methods. The problems outlined above and in the forthcoming article will undoubtedly become more severe as the number of torsional degrees of freedom increases. However, we believe that, where possible, the flexibility should be modelled as accurately as possible, and at the very least the charges should be determined from the most population conformation.

Conclusions

We have shown that the free energy perturbation method may be used to calculate log *P*s for ethanol and propanol (by assuming a log *P* for methanol). Although we have shown that propanol is more complicated than methanol or ethanol, it is likely that the methodology introduced here could be usefully used for higher members of the series. Absolute partition coefficients, as opposed to partition coefficient differences, can also be calculated using this methodology by growing the molecules from nothing.[50]

Further applications of the free energy perturbation method to calculate log *P*s could be very useful as the method could be applied to compounds whose experimental log *P* determination is difficult. In particular, we are currently applying the method to study the partitioning of a compound between an aqueous phase and a lipid bilayer as this is probably a more useful indication of biological activity than log *P*s in carbon tetrachloride or octanol.

The introduction of multiple conformation MEP charges represents a significant advancement in the use of free energy perturbation methods in applications such as this study of partition coefficients since it greatly enhances the ease with which the AMBER and related force fields can be extended beyond their original calibration set to study more flexible molecules. The additional computational cost of using multiple conformation MEP charges is linear in the number of conformations selected. We suggest that the decision as to whether this procedure should be used can be made by monitoring the dipole moment behavior as a function of conformation (see forthcoming paper). In this study, propanol turned out to be a particularly difficult molecule, and hence the extension of the log *P* calculations from methanol and ethanol to propanol was not routine. However, the results do show that the free energy perturbation method is a powerful tool and that reliable results may be obtained with care. Elsewhere, we have used the free energy perturbation method to make a systematic study of a variety of physico-chemical properties relevant to drug design, notably log *P*s, pK_as, electrode potentials, tautomeric equilibrium constants, and enzyme-ligand binding energies.[26,51] The routine application of free energy perturbation

(50) Cieplak, P.; Kollman, P. A. *J. Am. Chem. Soc.* **1988**, *110*, 3734–3739.
(51) Reynolds, C. A.; King, P. M.; Richards, W. G. *Mol. Phys.*, in press.

methods in this area is probably some way off, but the methods described here may well provide useful techniques for extending the range of applicability of the free energy perturbation and related methods.

Acknowledgment. J.W.E. wishes to acknowledge the support of Glaxo Group Research through the award of a Glaxo prize studentship. We wish to thank the Science and Engineering Research Council (SERC) for a grant of computer time on the CRAY XMP/432 at the Rutherford Appleton Laboratories and the SERC and IBM for time on the IBM 3090-600V under the strategic user initiative.

Registry No. CCl_4, 56-23-5.

Ab Initio Molecular Orbital Studies of the Rotational Barriers and the ^{33}S and ^{13}C Chemical Shieldings for Dimethyl Disulfide

Ding Jiao, Michael Barfield,* Jaime E. Combariza, and Victor J. Hruby*

Contribution from the Department of Chemistry, University of Arizona, Tucson, Arizona 85721.
Received September 6, 1991

Abstract: A series of ab initio molecular orbital calculations were carried out for dimethyl disulfide as a model for the disulfide bridges in proteins and peptides. The potential energy profile for rotation around the S-S bond was obtained at the HF/6-31G* level with full geometry optimization. Cis- and trans-barrier heights were estimated to be 11.40 and 6.27 kcal/mol, respectively, on the basis of fourth-order Møller-Plesset perturbation theory and 6-311G** basis sets. Calculations of the torsion angle dependence of the isotropic ^{33}S and ^{13}C NMR shieldings were based on the method of individual gauge for localized orbitals (IGLO). These are of interest for NMR studies of the disulfide bond in peptides and proteins. The minimum in the plot of ^{13}C shielding as a function of torsion angle occurs for a C1-S1-S2-C2 angle close to 110°, which is an optimum arrangement for lone pair back-bonding. An analysis of the paramagnetic bond contributions to the ^{13}C shielding at C1, for example, shows that the conformational dependence is dominated by the paramagnetic contributions to the C1-H1 bond, which points *away* from a lone pair on S2.

Introduction

The disulfide bridge is one of the two major covalent linkages between amino acids in polypeptides and proteins.[1] It has been known that disulfides in protein structures enhance the overall stability of some particular conformations.[2] In recent years, the use of conformational constraints has gained general attention in peptide synthesis.[3] In particular, disulfide formation has been used to limit the number of conformational states and to force β-turn-type conformations. Following current trends, which make use of molecular mechanics and molecular dynamics to study conformational property of peptides and proteins, refinement of force fields demands accurate experimental data, or high-level ab initio quantum chemical calculations for small but representative fragments of peptides and proteins.

In many experimental and theoretical studies dimethyl disulfide has been a model for the disulfide linkages in proteins or peptides.[4] Previous theoretical studies of dimethyl disulfide gave two energy barriers for rotation about the S-S bond. The trans-barrier is lower than the cis-barrier. The barriers create two minimum-energy conformations with C-S-S-C torsional angles near +90° or -90°. Although the geometry of $(CH_3)_2S_2$ was determined experimentally by microwave spectroscopy and by electron diffraction methods, the only known experimental value corresponding to an "effective rotational barrier" around the S-S bond is 6.8 kcal/mol from gas-phase thermodynamic studies.[5] This value has been taken as the trans-barrier height. There appears

Table I. Ab Initio Calculations of Torsional Barriers for Dimethyl Disulfide

methods	dihedral angles, deg	energy barriers, kcal/mol	
		cis	trans
STO-3G (rigid rotor)[a]	90	18.0	4.4
STO-3G* (rigid rotor)[a]	90	24.1	12.7
MB (rigid rotor)[b,c]	82.84	13.11	10.39
DZ (rigid rotor)[c,d]	86.23	16.03	9.16
STO-3G (opt)[e]	89.5	15.62	5.05
HF/4-31G//HF/STO-3G[e]	89.5	18.47	6.04
STO-3G[f]		12.68	6.27
DH+d[f]		16.49	8.00
HF/3-21G*//HF/3-21G*[g]	88.4 (opt)	11.97	5.69
HF/6-31G*//6-31G*[h]	87.29 (opt)	11.36	5.72
HF/4-31G*//HF4-31G*[i]	90 (fixed)	11.5	5.7
CI/4-31G*//HF/4-31G*[i]	90 (fixed)	9.4	6.0

[a] Boyd, R. J.; Perkynst, J. S.; Ramani, R. *Can. J. Chem.* **1983**, *61*, 1082-1085. [b] Minimum basis set: MB. [c] Pappas, J. A. *Chem. Phys.* **1976**, *12*, 397-405. [d] Double-ζ basis set: DZ. [e] Eslava, L. A.; Putnam, J. B., Jr.; Pedersen, L. *Int. J. Pept. Protein Res.* **1978**, *11*, 149-153. [f] Renugopalakrishnan, V.; Walter, R. *Z. Naturforsch.* **1984**, *39A*, 495-498. [g] Ha, T. *J. Mol. Struct.* **1985**, *122*, 225-234. [h] Reference 24. [i] Reference 29.

(1) Schulz, G. E.; Schirmer, R. H. *Principles of Protein Structure*; Springer-Verlag: New York, 1979.
(2) Thornton, J. M. *J. Mol. Biol.* **1981**, *151*, 261-287.
(3) Hruby, V. J. *Life Sci.* **1982**, *31*, 189-199. Hruby, V. J.; Al-Obeidi, F.; Kazmierski, W. *Biochem. J.* **1990**, *268*, 249-262.
(4) (a) For a microwave spectroscopic study, see: Sutter, D.; Dreizler, H.; Rudolph, H. D. *Z. Naturforsch.* **1965**, *20a*, 1676-1681. (b) For an electron diffraction study, see: Beagley, B.; McAloon, K. T. *Trans. Faraday Soc.* **1971**, *67*, 3216-3222. (c) For semiempirical quantum mechanical calculations, see: Van Wart, H. E.; Shipman, L. L.; Scheraga, H. A. *J. Phys. Chem.* **1974**, *78*, 1848 and references therein. For ab initio calculations, see Table I and quoted references.
(5) Hubbard, W. N.; Douslin, D. R.; McCullough, J. P.; Scott, D. W.; Todd, S. S.; Messerly, J. F.; Hossenlopp, I. A.; George, A.; Waddington, G. *J. Am. Chem. Soc.* **1958**, *80*, 3547-3554.

0002-7863/92/1514-3639$03.00/0